Fabrication of polymer electrolyte membrane fuel cell MEAs utilizing inkjet print technology

Silas Towne *, Vish Viswanathan, James Holbery, Peter Rieke

Pacific Northwest National Laboratories, Richland, WA 99352, United States

Abstract

Utilizing drop-on-demand technology, we have successfully fabricated hydrogen–air polymer electrolyte membrane fuel cells (PEMFC), demonstrated some of the processing advantages of this technology and have demonstrated that the performance is comparable to conventionally fabricated membrane electrode assemblies (MEAs). Commercial desktop inkjet printers were used to deposit the active catalyst electrode layer directly from print cartridges onto Nafion® polymer membranes in the hydrogen form. The layers were well-adhered and withstood simple tape peel, bending and abrasion tests and did so without any post-deposition hot press step. The elimination of this processing step suggests that inkjet-based fabrication or similar processing technologies may provide a route to less expensive large-scale fabrication of PEMFCs. When tested in our experimental apparatus, open circuit voltages up to 0.87 V and power densities of up to 155 mW cm^{-2} were obtained with a catalyst loading of 0.20 mg Pt cm^{-2}. A commercially available membrane under identical, albeit not optimized test conditions, showed about 7% greater power density. The objective of this work was to demonstrate some of the processing advantages of drop-on-demand technology for fabrication of MEAs. It remains to be determined if inkjet fabrication offers performance advantages or leads to more efficient utilization of expensive catalyst materials.
© 2007 Published by Elsevier B.V.

1. Introduction

Polymer electrolyte membrane fuel cells (PEMFCs) have emerged as promising future power sources for automobiles due to their high efficiency, high energy densities, modular construction, low operating temperatures and quick start-up capabilities [1,2]. However, large-scale application for automotive use requires transitioning an industry capable of producing a few thousand PEMFC stacks for both stationary and transportation applications, at a real cost of greater than $1000 kW^{-1}, to an industry capable of producing hundreds of thousand of stacks at a cost less than $50 kW^{-1}. Issues of durability and performance aside, reducing the manufacturing costs must involve reduced materials costs, especially as regards the PFSA membrane materials and the platinum catalyst content, and simplification of the membrane electrode assembly (MEA) fabrication process by reducing the number of processing steps.

Inkjet printers are well-known devices that utilize drop-on-demand technology to deposit various materials or "inks" without contact between the printer head and the substrate. This technology has become a popular manufacturing technique used around the world in desktop printers, and has been applied to deposition of various materials and the construction of unique devices such as ceramics, organic light emitting diodes, assembly of periodic structures, structural polymers and more [3,4].

Drop-on-demand printers use piezoelectric transducers – typified by the Epson (Nagano, Japan) line of home/office market printers – or thermal resistors – typified by the Canon (Tokyo, Japan) and Hewlett-Packard (Palo Alto, CA, USA) printers – to expel ink droplets only when needed. Both technologies print drops at a rate of one drop per 80–200 μs. This cycle time per drop includes initiating a current pulse to the respective plate to eject a droplet and refilling the ink cavity; the latter step consumes approximately 90% of the cycle time [5]. Nozzle sizes for these printers are usually 20–30 μm with ink droplets of 10–20 pL [3]. Technology is constantly improving to achieve better resolution with smaller nozzle sizes and ink droplets, with some printers delivering droplets as small as 1.5 pL. These

* Corresponding author. Tel.: +1 509 372 6563; fax: +1 509 375 2167.
  E-mail address: silas.towne@pnl.gov (S. Towne).

printers offer high resolution (dots per inch), as well as the ability to print intricate features, gradients, and 3D structures in a repeatable manner. Recently "memjet"-based printer systems have been touted for their very high print speeds [6].

In addition to drop-on-demand systems, there are also continuous inkjet systems that use an electrostatic field to direct the flight of ink droplets. It has been proposed by Le [5], in his review of inkjet technology, that drop-on-demand systems have replaced many of the continuous jet printers, especially in the home/office market. In industrial applications where a given product, such as an MEA, may be produced in multiple quantities, it is not clear that drop-on-demand necessarily holds advantages over more continuous printing or coating techniques.

Some of the essential criteria for MEA fabrication are (1) the reduction in the number of processing steps required to fabricate the MEA, (2) wherever possible have continuous rather than batch processing from material input to stack assembly, (3) adaptability to fabricate different MEAs (e.g. compare the catalyst layer composition needed for a direct methanol fuel cell, pure hydrogen-based and reformate-based fuel cells), (4) the ability to rapidly change size, shape and quantity of MEAs produced, (5) very high product quality control with the associated manufacturing metrics and (6) be capable of production speeds matching (but not necessarily greatly exceeding) that of other rate-limiting fabrication and assembly processes.

The relatively high complexity of drop-on-demand fabrication must be contrasted to the simplicity of roll coating. Inkjet fabrication is much more versatile than roll coating in the ability to transition from one small- or medium-scale job to the next job. In comparison, roll-coating facilities are difficult to set-up and optimize for a given job and are better suited to large-scale, high-speed production. Further, inkjet fabrication allows the deposition of complex structures or if you will, "images". For example, it is critical to optimize the performance of the MEAs while minimizing the Pt loading. Progress has been made in this area as many researchers have demonstrated the reduction of Pt loadings from greater than $4 \, \text{mg cm}^{-2}$ to $0.4 \, \text{mg cm}^{-2}$ without loss in performance [7–9]. However, with increased control during manufacturing, precision-deposited Pt catalyst could further reduce Pt loading while maintaining power density and durability [10]. This can be accomplished by grading the loading within the thickness of the catalyst layer but it may also prove useful to vary the loading density from fuel or oxidant inlet to outlet ports.

Another important attribute of drop-on-demand-based manufacturing is the exceptional reproducibility combined with the unique ability to adapt the manufacturing process to evolving designs or applications. This characteristic may be used to achieve the very low cell failure rates needed to maintain acceptable levels of failure in assembled stacks. Further, an individual fabrication line can be readily adapted from production of MEAs required for automotive applications to that required for stationary power applications and even to direct methanol applications. Large-scale inkjet printers can utilize multiple cartridges capable of holding a variety of solutions (various "colors") for changing applications or for variation of MEA composition as well as across a specific printed electrode area. In addition, scaled up inkjet printers will still have the ability to instantaneously change printing patterns, sized resolutions and thicknesses without major retooling or setup. Although many technologies may lose their adaptability and versatility when scaled up, inkjet technology provides versatility useful in small-scale single run MEA design development to medium-scale job-shop production runs to large-scale dedicated fabrication lines.

Parameters that impact the utility of inkjet print technology specific to a component include the inkjet array delivery capabilities, the environment in which the unit operates, the system precision, and the functional control of the entire manufacturing process. One critical step in this process is the formulation of the colloidal suspension delivered to the substrate, including the composition and stability over the manufacturing process time span. Ink composition must meet rigid requirements to maintain uniform print patterns and prevent clogging of the printer nozzles by dried ink or large particles. The most important parameters are the ink viscosity and surface tension, as well as particle size. The energy of each printed drop must be sufficient to overcome the viscous flow and surface tension of the ink, yet the viscosity must be low enough to allow the ink reservoir to refill quickly. In addition, if the ink surface tension is not high enough in the nozzle, it will spontaneously drip [3]. In combination with dripping, lower surface tension can lead to wetting of the faceplate around the nozzle preventing formation of a stable droplet stream and ultimately causing drying around the nozzle [3]. Drying will cause nozzles to become blocked and no longer functional. Thus, humectants, low volatility water-miscible liquids such as ethylene glycol, are added to prevent drying [3].

Typically, inks are designed to match the desired performance of a particular printer (or vice versa), so novel solutions must meet ink properties specific to the given printer before successful printing can be accomplished. For the inks tested from printers in the home/office market, these properties are a viscosity between 1 cP and 4 cP, surface tension in the range of $30–35 \, \text{mN m}^{-1}$, and an average particle size of approximately $0.2 \, \mu\text{m}$.

When printing colloidal solutions, sedimentation must be avoided and particle sizes should ideally be at, or preferably less than, $1 \, \mu\text{m}$ for typical desktop printers. Large particles, agglomerated particles, settling of unstable colloids, or even dust clog the nozzles, increase the viscosity and lead to short ink shelf-life [3]. Other necessary characteristics of inkjet compatible inks are the ability to correctly wet the substrate, be quick drying, smear resistant, and permit easy clean-up with limited maintenance [5].

The primary objective of this study was to create print solutions that exhibit the above characteristics, while optimized for fabrication of highly functional MEAs. The key to a successful MEA is creating an ideal three-phase boundary, a network of electrical and ionic conductivity with adequate porosity to allow the transport of gas, protons and electrons throughout the networks. Previous research has focused on the optimization of this region through ideal ionomer to Pt/carbon ratios, fabrication techniques, and selective conditioning processes of the membrane and finished MEA [8,10–13]. In our study, inkjet technology was utilized to print layers of catalyst solutions directly on the membrane. Despite the use of the membrane

in proton form, a highly adherent, mechanically stable catalyst layer could be formed without any hot pressing process [14,15]. The electrochemical properties of the electrodes were compared for various processing conditions and compared to commercially available MEAs. Our purpose was not to demonstrate superior or state-of-the-art electrochemical performance but to show that inkjet-printed MEAs showed comparable performance to commercially available MEAs while offering some distinct processing advantages.

2. Experimental

2.1. Catalyst formulation

Catalyst solutions were prepared by thoroughly mixing a carbon-supported catalyst (Vulcan XC-72R, E-TEK, Somerset, NJ) with Nafion® solution (EW1100, Ion Power Inc., New Castle, DE) and Milli-Q grade de-ionized water. Water, ethylene glycol and isopropanol were added to adjust the viscosity and surface tension. To form a homogeneous ink, the solutions were sonicated (Branson Sonifier) for 5 min and stirred with a magnetic stir bar for 24 h. A design of experiments protocol was used to select ink compositions that were compatible with the desktop printer used in this study. For each ink composition, the particle size (Horiba Laser Scattering Particle Size Distribution Analyzer LA-920), viscosity (Kruss K12 tensiometer) and surface tension (Bohlin VOR Rheometer) were determined, followed by an actual printing test. While the print quality, as determined by the durability, continuity (lack of visual banding within the printed layer) and smearing of the image or by clogging or caking of the print head, was subjective, this method resulted in high quality, stable inks that printed well. As expected, it was determined that the ink with the best printability had similar attributes to commercial inks designed for a specific printer. Good inks also maintained colloidal stability for at least a few days.

2.2. Preparation of Nafion® membranes

Nafion® membranes (N117, Ion Power, Inc.) were washed for 1 h in 3 wt% H_2O_2, rinsed and boiled for 1 h in de-ionized water, boiled in 0.5 M H_2SO_4 for 1 h, rinsed, and boiled in de-ionized water for 60 min [17]. The membrane was then stored in Milli-Q grade de-ionized water until ready for use. Just prior to printing, the membrane was gently dried on a vacuum table under low heat (under 70 °C) until wrinkle free and the membrane had returned to its original dimensions.

2.3. Printing of catalyst inks on Nafion® membranes

Off-the-self piezo (Epson) and thermal (HP) inkjet printers were used with only minor modification. The ink cartridges were opened, cleaned of the original ink and filled with the catalyst ink using a syringe. All ink was removed from the neighboring cartridges to remove the possibility of contamination. The membrane was secured to a cellulose acetate sheet and fed through the printer using the original paper feed platen. Illustrator software was used to control the print parameters.

Electrode dimensions were changed by altering the shape and size of the bitmap image on the computer. Electrode thickness and resolution were controlled by modifying the hue, saturation and luminescence. These parameters are directly related to the drop delivery rate and spacing but this relationship is not available from the manufacturer.

Up to 24 successive layers of varying compositions were printed to build the desired electrode structures. Printing was conducted at ambient room temperature and under these conditions, less than 1 min was required to achieve adequate drying between prints and was determined primarily by the time taken to re-align and reload the sample. After all layers were printed the electrode was dried by gently warming with a heat gun for less than 30 s. The substrate was then turned over and re-secured to the acetate medium, and the printing and drying processes repeated.

The printed electrodes were then processed by a variety of procedures that included hot pressing at various temperatures and water extraction. Water extraction removes the ethylene glycol ink carrier while hot pressing was used with the intention of improving the integrity and adhesion of the films.

2.4. Preparation of MEA sample for conductivity, optical micrographs, and SEM and TEM measurements

To measure the electrical conductivity, a single layer was printed on cellulose acetate using a grey scale to vary the amount deposited. The resistivity as a function of thickness of the layer was measured using a Seebeck Measurement System (MMR Technologies, Inc., Mountain View, CA). This same density gradient was also viewed top down through an Olympus SZH stereozoom microscope (Center Valley, PA) with an attached PAXcam digital microscope camera (Villa Park, IL) to obtain optical micrographs.

For SEM, 20 mm × 5 mm samples were cut from the middle of the MEA and the cross-section was examined using a JEOL VSM-5900LV scanning electron microscope. TEM sample preparation consisted of cutting a small sample, embedding the sample in epoxy resin and curing overnight at 60 °C, then sectioning with a diamond knife via an ultra-microtome at room temperature. The 100 nm sections were subsequently examined in a JEOL 2010 high-resolution TEM equipped with 200 kV acceleration voltage equipped with an energy dispersive spectroscopic (EDS) detector.

2.5. Fuel cell performance measurements

MEAs produced for this study were compared to commercially available MEAs. Initial tests were conducted using a LightFC-1 (Fuel Cell Store, Boulder, CO) single cell fuel cell test system, designed for demonstration and low power output performance and with 2.75% H_2 (97.25% Argon) at flow rates of approximately 0.2 L min^{-1} and air at rates of approximately 0.05 L min^{-1}. Later studies used an in-house fabricated cell and 100% H_2 (35 mL min^{-1} and 50 mL min^{-1}) and air. The system was operated between ambient temperature and 75 °C, with peak performance occurring at 75 °C.

In all cases, both gases were 100% humidified using an Immersion Circulator (VWR model 1112A) to control the temperature of the water bath and Perma Pure MD Gas Humidifiers to humidify the gases. Three way valves were utilized for both the hydrogen and air gas lines allowing the selection of either humidified or non-humidified gas streams. Carbon cloth backings (GDL ELAT 1200-W, Fuel Cell Store) were used as gas diffusion layers. Commercial MEAs tested were three-layer MEAs (SL-117, Fuel Cell Store) with loadings of 0.3 mg cm^{-2} Pt for both the anode and cathode on Nafion$^{®}$ 117 membranes.

To test the performance a load bank was used consisting of resistors in the 0.1–20 Ω range. By connecting various resistances across the fuel cell, the current was varied, and a *V–I* curve generated. The current was measured by a digital multimeter connected in series with the circuit, while the voltage was measured directly across the fuel cell terminals by another digital multimeter.

3. Results and discussion

3.1. Ink compatibility

While no best ink was identified, suitable inks have better than 98% of the particles with a size less than 2 μm. Fig. 1 shows the particle size distribution of a typical ink suitable for printing. Though this ink showed greater particle size disparity and a larger average size than commercial inks, the ink maintained colloidal stability and consistently passed through the cartridge filter and print head. The surface tension of this ink was 35.5 mN m^{-1}. This value is at the high end of the range found for commercial inks (30–35 mN m^{-1}). Finally, the viscosity was found to be 3.35 cP, again within the range of the OEM inks (1.5–4 cP).

Suitable ink characteristics are governed by the print head design and operation and are not necessarily related to the best electrode composition. A drawback to off-the-shelf systems is this limited range of suitable ink characteristics. More advanced printing systems that might be used in large-scale MEA fabrication have a much wider range of suitable ink characteristics.
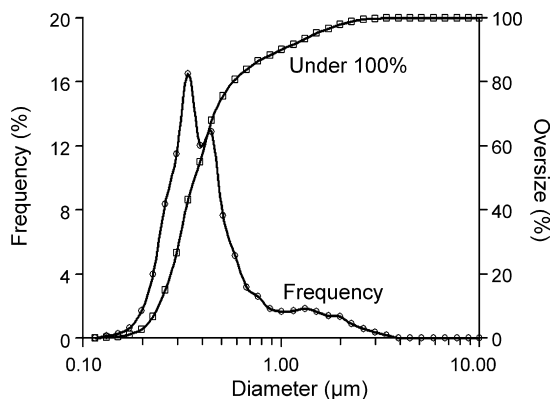

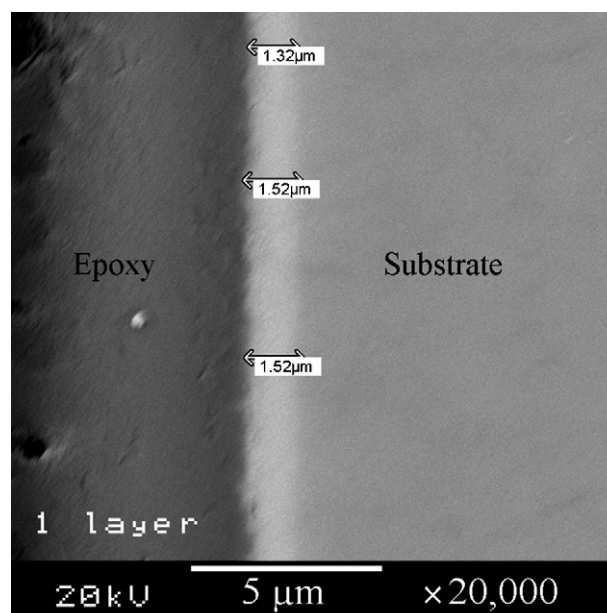Fig. 1. Particle size distribution of catalyst solution after sonication and stirring.

Fig. 2. SEM cross-section of a single catalyst layer on a cellulose acetate substrate. The arrows measure the thickness of the catalyst layer at their prospective location. To the right of the catalyst layer is the substrate. To the left is epoxy (dark grey).

3.2. Membrane/electrode assembly

Fig. 2 replicates a cross-section SEM image of a single catalyst layer, approximately 1020 nm thick, printed on a cellulose acetate substrate. Depending upon the printer system, layers as thin as 400 nm could be printed. Providing the mass of materials deposited was sufficient, the layers were of very uniform thickness over large areas with a variation in thickness of a few percent and a roughness much smaller than the thickness of the films. When insufficient material was deposited, the print drops did not fully coalesce and showed a pattern consistent with the drying of single drops. These results demonstrate the potential of drop-on-demand technology to print evenly distributed catalyst layers as desired and shows the importance of substrate wettability on the distribution of material.

The conductivity was characterized at various locations to determine if the carbon network was deposited in an effective manner. In addition to the above printed layer, conductivity measurements were also compared for various thinner printed layers. The total ink density was controlled by changing the luminescence on the illustrator program in approximately 4% increments for each layer. Increasing the luminescence creates a lighter image that reduces the amount of ink deposited, resulting in a thinner layer. In all, 14 different thicknesses were printed and all deposits were clearly visible and the optical density as determined qualitatively by eye correlated with the luminescence setting.

As seen in Fig. 3, the resistivity was about 1 Ω cm for thicknesses above 580 nm, indicating reasonable connectivity throughout the layer. Below this thickness the resistivity rapidly increased into the mega ohm range and was too high to be accurately measured. These results suggest that segregation of the
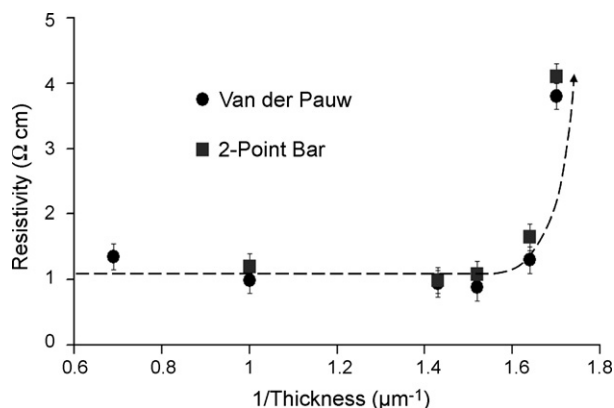
Fig. 3. Variation of resistivity of carbon supported catalyst layer with film thickness on cellulose acetate support.
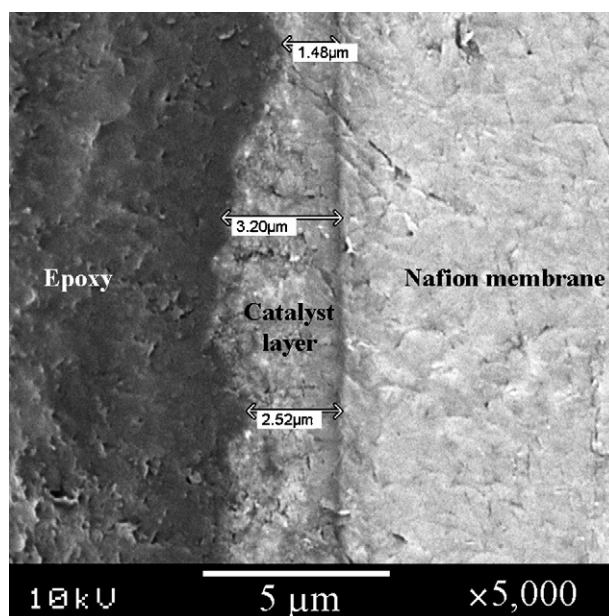

Fig. 5. SEM cross-section of eight printed catalyst layers on Nafion®. The catalyst layer is labeled in the middle with the membrane on the right and epoxy on the left.

carbon occurred, or because of the printer characteristics, the material was not uniformly distributed. With this particular printing system, a deposit of at least 1 μm was required to maintain good electrical conductivity.

By using a commercially available printer, printing parameters such as droplet size, jetting velocity, print head speed, number of nozzles, distance between nozzles, and platen speed cannot be manually controlled. Therefore, without exact matching to the OEM inks, some discontinuities will occur. In this study, evidence of banding appeared when printing a single layer. Banding occurred when drops printed in one pass of the print head do not coalesce with the next print pass. With higher dpi (dots per inch) and low luminescence the appearance of banding lessened. Also, with the printing of additional layers these lines disappeared as ink fills in the areas with less ink. Fig. 4 shows 3 of the 14 single layers printed to test conductivity. Fig. 4a represents the lowest luminescence and therefore, the highest thickness and best connectivity of the 14 samples. In the figure there is still some evidence of banding, but there was adequate connectivity to give a negligible resistivity. Fig. 4b represents the seventh thickest print, a print that had low conductivity. Less connectivity is seen in this figure as the drop overlap in both the vertical and horizontal direction lessens. In Fig. 4c, the sample with the highest luminescence, and therefore the thinnest of the samples, showed the greatest degree of discontinuity. Individ-

ual droplets start to become visible and there is no recordable conductivity.

As expected, printing on Nafion® proves to be more difficult than cellulose acetate as commercial printers are optimized to match the print speed to specific ink and substrate characteristics. Another issue with Nafion® is swelling of the membrane from the water and alcohol in the catalyst ink. Water alone can swell the membrane by as much as 32%, causing an uneven printing surface [16]. Fig. 5 shows a cross-section SEM image of eight catalyst layers printed directly on Nafion®. A thickness of up to 3.2 μm was measured. This first generation of printed MEAs had a much thinner electrode thickness than the 10–20 μm thickness typical of commercially available electrodes. In additional work much thicker electrodes were deposited. It is apparent from these results that inkjet printing allows excellent control over the individual layer thickness but still allows many layers and ultimately much thicker electrodes to be deposited.
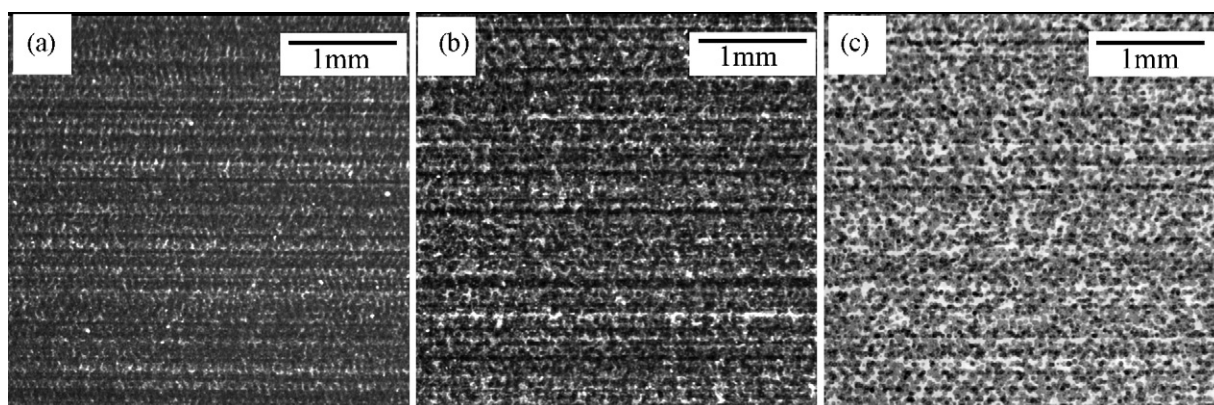

Fig. 4. Optical micrographs taken at 15× magnification showing evidence of banding in three samples of different thickness (drop amounts): (a) high, (b) medium, and (c) low. (a) has high conductivity whereas both (b) and (c) have no conductivity due to low connectivity.
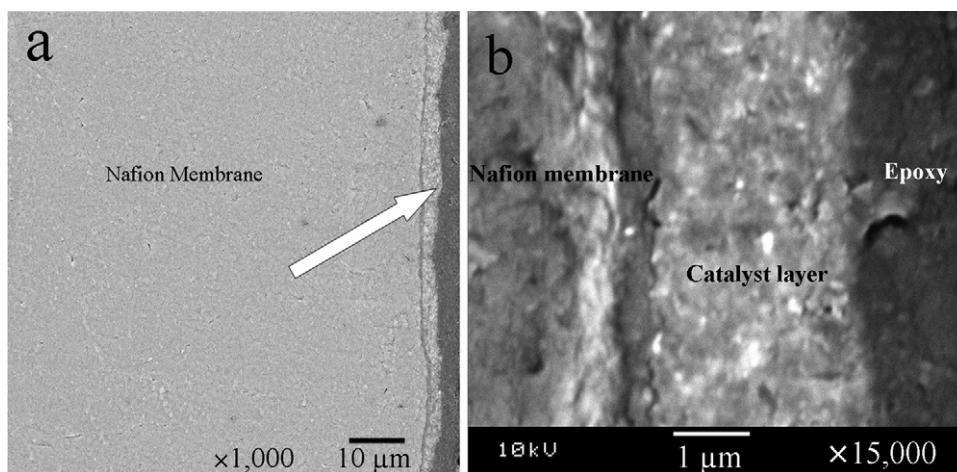
Fig. 6. SEM cross-section of eight printed layers on Nafion® cured in oven for 10 min at 120 °C. The catalyst layer is represented with an arrow with the Nafion® membrane on the left and epoxy on the right. The scale bars represent (a) 10 μm and (b) 1 μm.

Also visible in the cross-section of the MEA is a thin dark line located at the interface of the membrane and the catalyst ink. With no processing on the MEA, such as hot pressing, the catalyst layer is adhered to the membrane but not mechanically embedded. This gave rise to concerns about the mechanical adhesion of the catalyst layer to the membrane. Fig. 6a and b represent a cross-section view of Pt/C on Nafion® and cured in an oven for 10 min at 120 °C to promote evaporate the residual alcohols. Fig. 6a shows a magnification at 1000×, showing the good consistency of the catalyst layer over large areas. In this image the Nafion® membrane is on the left separated from the catalyst layer by a thin dark line. The darker grey and black areas represent epoxy. A magnified view of this MEA is depicted in Fig. 6b, with a thin dark line again separating the Nafion® on the left from the catalyst layer. These SEM images of the MEA cross-section indicate the catalyst layer is uniformly continuous and is adhered to the membrane with no evidence of delamination.

The nature of the materials comprising the thin dark line at the interface between the catalyst layer and the membrane could not be identified. As this line appeared darker in the SEM, it could be presumed to be more electrically conductive than the adjoining regions and this could be explained by phase segregation of carbon particles to the interface. The answers to questions of how this occurs and whether this effect is responsible for enhanced adhesion will have to await further study.

To test adhesion, MEAs were subjected to mechanical and chemical treatments. Catalyst layers remained adhered even through boiling in water or sulfuric acid. No significant amount of material was removed by the simple yet standard scotch tape peel test. Bending of the sample did not result in flaking nor did light rubbing with a tissue. The catalyst layer could be visibly damaged by a determined scratch such as with a finger nail or sharp object. From this we determine that the adhesion is more than sufficient for assembly of a cell without mechanical damage to the catalyst layer. We note that this is achieved with no chemical modification of the Nafion® membrane – such as conversion to the sodium form – prior to printing and without any

hot pressing after deposition as is typically used in MEA fabrication. The effect of hot pressing is discussed below. We also note here that the MEA remained mostly intact upon disassembly of the cells after electrochemical testing. However, some parts of the catalyst layer adhered to the gas diffusion layers or to the gas manifold.

Figs. 5 and 6a show that printing on Nafion® results in some slight in-homogeneities within the catalyst layer thickness. This is due to both the uneven surface and the effect of swelling when printing on a Nafion® membrane, as well as the lack of ability to control the operating conditions of a commercial printer. Possible improvements with a commercial printer can be made with an improved technique for securing the membrane to the printer roller base during printing or by using reinforced membranes to minimize the effects of swelling. With reduction of swelling the catalyst layer printed on the Nafion® membrane should mimic that of the cellulose acetate substrate, resulting in an even catalyst layer surface.

Further analysis of the MEA with TEM shows an incomplete carbon network as seen in Fig. 7a and b. The cross-sectional view in Fig. 7b shows carbon particles with diameters of approximately 100 nm and catalyst particles between 3 nm and 10 nm (represented by black dots). The MEA represented in these pictures has not been hot pressed and represents the as-printed condition. The carbon particles in Fig. 7a do not show the continuity expected from the SEM images. Instead, there is clear evidence of a layered morphology of alternating layers of approximately 0.5 μm thickness. It is hypothesized that the two differing layers are a carbon–ionomer layer and a layer of residual ethylene glycol, both deposited with a single print of the inkjet printer. Each successive print therefore adds two additional differing layers with a similar morphology.

Without a continuous carbon–ionomer network, both the electronic and ionic conductivities will decrease and presumably detrimentally affect the electrochemical performance. Different techniques for removing this impeding layer of ethylene glycol were tried. These included hot pressing at various temperatures to compact and strengthen the catalyst layer and using water
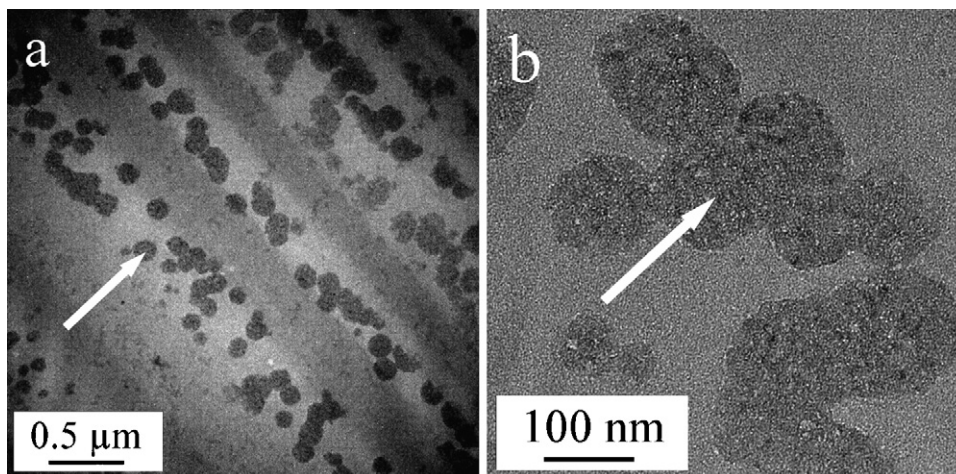
Fig. 7. TEM image of printed catalyst layers on Nafion® before processing. The arrow represents carbon particles. The small black dots on the carbon are platinum particles. The scale bars represent (a) 0.5 μm and (b) 100 μm.

extraction to remove the ethylene glycol as seen with glycerol removal in previous studies [17]. As earlier discussed, this study compares hot pressing with water extraction as well as with the combination of water extraction and hot pressing.

Fig. 8a and b shows images of an MEA pressed at 2045 psi for 5 min at 125 °C. Clearly the interconnectivity of the carbon has been increased over that shown in the previous figure. These samples showed increased electrical and ionic conductivity within the section, as well as evidence of the porous network. The black dots within the image represent the Pt on the darker grey carbon particles. After pressing there is no longer evidence of the layers seen in Fig. 7a. The ethylene glycol was assumed to be at least mostly removed by heating. It was expected that with the improved electrode structure seen after hot pressing, that performance of the MEA would also increase.

In summary, the MEAs depicted in these images are relatively uniform and repeatable, showing porous and distributed three-phase boundaries manufactured by printing catalyst layers via an automated process. Using only a modified commercially purchased printer, these results show the merits of drop-on-demand manufacturing as a precise, repeatable, and potentially more cost effective process as compared to other MEA manufacturing techniques.

3.3. Performance of single cells

Fuel cell performance was measured on fabricated MEAs with printed layers for both the anode and cathode. The active area of each printed MEA was $2.25 \, cm^2$. With the commercial printer an optimized dpi of 2880×1440 was printed. Over a print area of $1.5 \, cm \times 1.5 \, cm$ about 1.4 million drops were printed for each layer with a drop size of 3 pL [18]. From this the Pt loading can be determined and the MEAs used for electrochemical test described below have a platinum loading of $0.094 \, mg \, Pt \, cm^{-2}$ unless otherwise noted. For laboratory safety reasons only 2.75% H_2 could be used for these initial studies. While this does not give optimal results that allow detailed comparison of different electrodes it did allow evaluation of the effects of processing on electrode performance.

Testing began by measuring the $I-V$ response of the MEAs with no processing. Two separate printed MEAs gave nearly identical results when tested with no post-processing as exem-
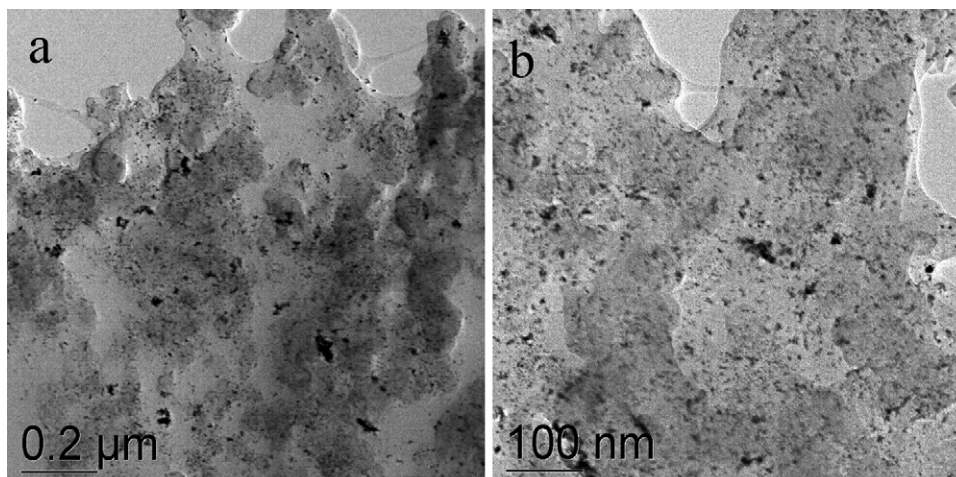

Fig. 8. TEM image of printed catalyst layers on Nafion® after pressing MEA at 2045 psi at 125 °C for 5 min. The scale bars represent (a) 0.2 μm and (b) 100 nm.
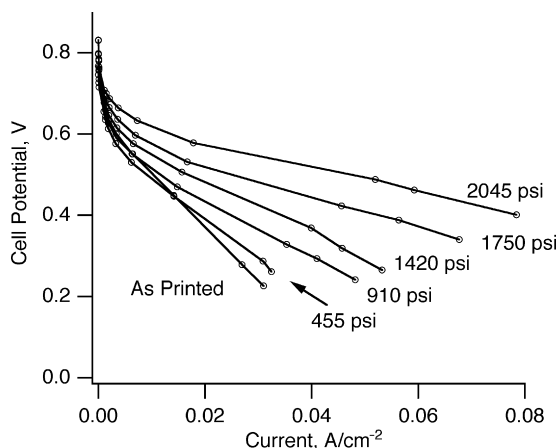
Fig. 9. Polarization curves comparing printed MEAs hot pressed at various pressures for 5 min at 125 °C to an unprocessed MEA. Cells were tested with 2.75% H$_2$/air at 75 °C, ambient pressure and 100% RH.

Fig. 11. Polarization curves comparing printed MEAs water soaked and water soaked and hot pressed at various pressures for 5 min at 125 °C to an unprocessed MEA. Cells were tested with 100% H$_2$/air at 75 °C, ambient pressure and 100% RH.

plified by the baseline curves in Figs. 9 and 10. In Fig. 9, the current density as a function of cell voltage of a MEA with no post-processing is compared against hot pressing at different pressures at 125 °C for 5 min; all tested at 75 °C and with 2.75% H$_2$/Ar and air. Hot pressing at a temperature of 125 °C made a large difference in improving the performance of the printed MEAs. Higher current densities at all voltages were seen with each increase in pressure reaching a maximum with a pressure of 2045 psi. This indicates that specific hot press pressures and temperatures have a significant and positive effect on the catalyst layer structure and improve MEA performance and power density. This experiment was also done with pressing at 100 °C, but showed very different results. No performance gain was achieved with pressing, indicating elevated temperatures are needed to compact the catalyst layers and improve the electrode performance. After a pressure of 2045 psi and 125 °C, the membrane delivered a maximum output of 78.5 mA cm^{-2} at 0.401 V, representing a power of 31.5 mW cm^{-2}. This was due to increased contact between the catalyst and the membrane and compression of the multiple printed layers to form a more continuous carbon network as seen in Fig. 8a and b. Apparently
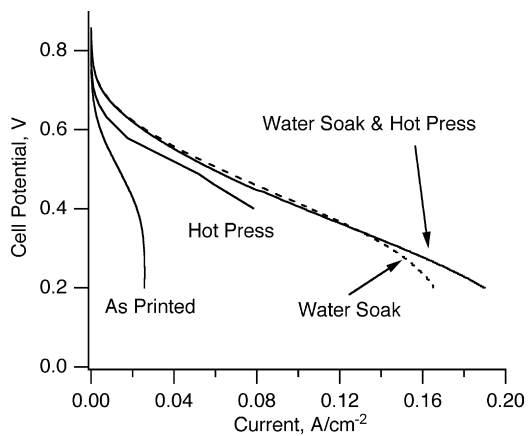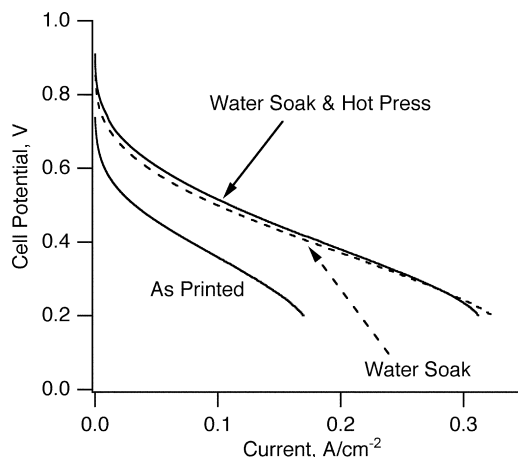

Fig. 10. Polarization curves comparing printed MEAs water soaked and/or hot pressed at various pressures for 5 min at 125 °C to an unprocessed MEA. Cells were tested with 2.75% H$_2$/air at 75 °C, ambient pressure and 100% RH.

a combination of sufficient temperature and increasing pressure squeezes the ethylene glycol from the catalyst layer. Presumably some ethylene glycol remained in the catalyst layer.

In Fig. 10, the I–V response of another MEA with no processing is compared to a MEA soaked in water to leach out ethylene glycol. Also compared in Fig. 10 is a MEA that is first soaked in water and then pressed at 950 psi for 3 min at 125 °C. What can be learned from Fig. 10 is that water leaching of the ethylene glycol is superior to just simple hot pressing at elevated temperatures and pressures. For a direct comparison to hot pressing, the soaked MEA delivered 106 mA cm^{-2} at 0.401 V, representing a power of 42.4 mW cm^{-2}. This represents nearly 35% improvement over the power output of the MEA with only hot pressing and no water extraction. The soaked MEA recorded a maximum power output of 44.5 mW cm^{-2} at 0.340 V. The MEA soaked and pressed recorded a power of 44.6 mW cm^{-2} at 0.340 V and a maximum power output of 45.0 mW cm^{-2} at 0.324 V. This shows that hot pressing in addition to water extraction leads to very little if any additional electrochemical improvement over just water extraction. This is important as hot pressing not only adds an additional manufacturing step, but also can permanently damage the proton exchange membrane leading to reduced durability and lifetime of the MEA.

Electrodes soaked in hot water continued to show excellent adhesion even without a hot press step. Given the discontinuous layered structure shown in Fig. 7, this was an unexpected result. Rather it was expected that water extraction would result in extensive delamination of the interface and that hot pressing would be a necessary first step. This was not the case and at this time we cannot offer a good explanation for this advantageous result.

After determining that water extraction was superior to just hot pressing, the samples from Fig. 10 where tested using 100% H$_2$ and air to make a better comparison to commercial MEAs. As can be seen in Fig. 11, use of 100% H$_2$ dramatically improves the performance of all MEAs. These curves translate into peak performance of 77.4 mW cm^{-2} at 0.350 V for the soaked MEA
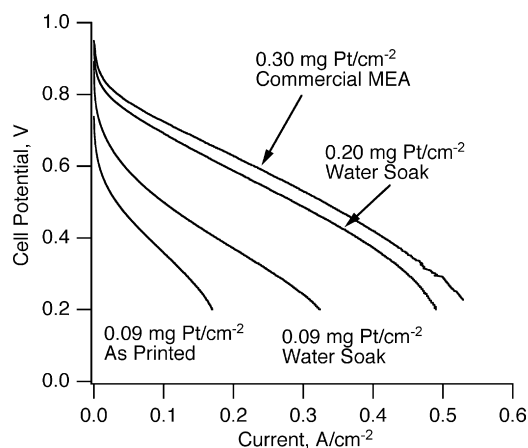
Fig. 12. Polarization curves comparing a commercial MEA with printed MEAs with different processing techniques and different loadings. Cells were tested with 100% H_2/air at 75 °C, ambient pressure and 100% RH.

and 78.9 mW cm^{-2} at 0.332 V for the soaked and pressed MEA. This represents nearly a 75% increase in peak power for both curves using 100% H_2 over 2.75% H_2.

After comparing the effects of processing for the MEAs, the fabricated membranes were compared against a commercially sold MEA tested using 100% H_2 and air. Fig. 12 reports current density as a function of input voltage of the following four selected MEAs: (1) the printed membrane with no post-processing and 0.094 mg Pt cm^{-2} for anode and cathode, (2) the printed membrane soaked in water to extract ethylene glycol with a loading of 0.094 mg Pt cm^{-2}, (3) a printed membrane with just over twice the amount of printed layers to give a loading of 0.20 mg Pt cm^{-2}, also soaked in water to extract ethylene glycol, and (4) the commercially fabricated membrane with a loading of 0.3 mg Pt cm^{-2}. Fig. 13 compares the power densities versus cell voltage for the same four MEAs. In these figures it can be seen that though the commercial MEA significantly outperformed the MEA with a much lower catalyst loading, the printed MEA with 0.2 mg Pt cm^{-2} has a comparable maximum power density to the commercial MEA. The commercial MEA recorded a peak performance of 365 mA cm^{-2} at 0.462 V, repre-

senting a power density of 167 mW cm^{-2}. At that same voltage, the printed MEA recorded a performance of 333 mA cm^{-2} and a power density of 154 mW cm^{-2}. The printed MEA reached a maximum power density of 155 mW cm^{-2} at 0.459 V. Therefore, with a 33% reduction in catalyst loading compared to the commercial MEA, the printed MEA recorded only a 7% lower peak power density.

These results show that despite a lower catalyst loading, inkjet-printed MEAs can compete with commercially available MEAs. The MEAs tested also had very similar polarization curves, representing similar resistive losses, including kinetic, ohmic and mass transport losses within the fuel cell system. This is important as both systems were tested with the same GDLs, gas concentrations, humidity, and Nafion® membrane thickness. We do not represent these results as indicating optimal performance for either the printed or commercial electrodes. We made only the requisite effort to assure the membranes were adequately hydrated. Operation at 75 °C was convenient but not necessarily ideal. Obtaining optimal electrochemical performance requires considerable effort and that was not the objective of this work. Rather, we have demonstrated that inkjet fabrication offers significant processing advantages and appears to offer comparable electrochemical performance.

4. Conclusion

A new method for fabricating MEAs for PEMFCs has been developed using relatively inexpensive home or office type inkjet printers to deposit successive layers of Pt/C catalyst dispersed in an ink-like solution. Nafion® is attached to a support and fed through the printer where the catalyst is printed in an even and repeatable manner to produce uniform catalyst layers. With an active electrode area of 2.25 cm^2, the cell has been operated up to current densities of 155 mA cm^{-2} with a loading of just 0.20 mg Pt cm^{-2}. These results are within 10% of a commercial membrane while operating with 33% less catalyst loading and while only in the initial stages of production. This novel fabrication technique, as an automated process, is both simple and time effective and has the potential for scaling to larger production techniques while still sustaining the ability to structure MEA electrodes.

Our objective here was to demonstrate in a simple manner the basic process of inkjet fabrication of MEAs. Clearly there are remaining questions concerning the economics, speed and reliability of this method compared to established methods. For example, roll-coating techniques would be simpler for large-scale production of MEA with very simple morphologies and compositions. However, inkjet fabrication can be the basis of a more agile and flexible manufacturing method that can be adapted to various sizes of MEA and/or compositions. Further, inkjet fabrication can allow the precise location of costly platinum catalyst both through the thickness of the catalyst layer and from gas inlet to outlet. This represents a potential for significant reduction in overall catalyst loading by optimizing the local density of the catalyst. That is a process not easily achieved through roll-coating techniques. Finally, we re-emphasize that the meth-
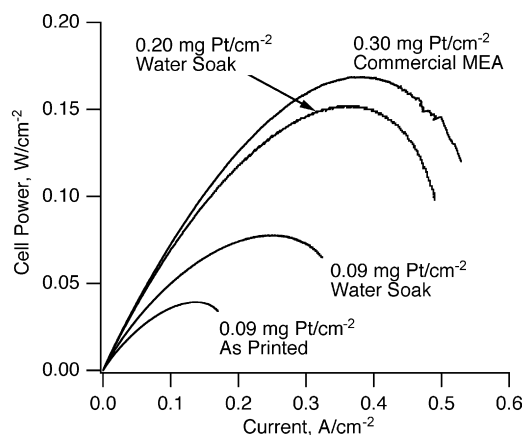

Fig. 13. Power curves comparing a commercial MEA with printed MEAs with different processing techniques and different loadings. Cells were tested with 100% H_2/air at 75 °C, ambient pressure and 100% RH.

ods presented here offer substantial simplification of the overall MEA fabrication process. We need make no use of chemical conversion to the membrane and do not require any hot pressing operations. However, it remains to be demonstrated that inkjet-based fabrication can equal or better the performance of MEA fabricated by now current well established, well understood and optimized processes.

In initial assessments, fabrication of PEM fuel cells with inkjet technology has proven to be very promising. With the first generation of printed and processed MEAs, power densities of fabricated cells are close to that of commercial MEAs in our fuel cell test apparatus. Future experimental work will focus on better understanding the three dimensional structure of a printed electrode and building new structures with inkjet technology to improve electrode efficiencies while reducing costs compared to electrodes made with previously known techniques [8,10,12].

Acknowledgments

References

[1] D. Bevers, N. Wagner, M.V. Bradke, Int. J. Hydrogen Energy 23 (1988) 57.
[2] V. Mehta, J.S. Cooper, J. Power Sources 114 (2003) 32.
[3] P. Calvert, Chem. Mater. 13 (2001) 3299.
[4] James E. Smay, Joseph Cesarano III, Jennifer E. Lewis, Langmuir 18 (2002) 5429.
[5] H.P. Le, J. Imaging Sci. Technol. 42 (1998) 49.
[6] Anon, Economist.com, 2007.
[7] E.A. Ticianelli, C.R. Derouin, S. Srinivasan, J. Electroanal. Chem. 251 (1988) 275.
[8] M.S. Wilson, S. Gottesfeld, J. Appl. Electrochem. 22 (1992) 1.
[9] M.S. Wilson, S. Gottesfeld, J. Electrochem. Soc. 139 (1992) L28.
[10] M.S. Wilson, J.A. Valerio, S. Gottesfeld, Electrochim. Acta 40 (1995) 355.
[11] G.S. Kumar, M. Taja, S. Parthasarathy, Electrochim. Acta 40 (1995) 285.
[12] M. Uchida, Y. Aoyama, N. Eda, A. Ohta, J. Electrochem. Soc. 142 (1995) 463.
[13] Wilson, M.S., Membrane catalyst layer for fuel cells, US Patent 5,234,777 (1993).
[14] Y.-G. Chun, C.-S. Kim, D.-H. Peck, D.-R. Shin, J. Power Sources 71 (1998) 174.
[15] S.S. Kocha, in: W. Vielstich, H.A. Gasteiger, A. Lann (Eds.), Handbook of Fuel Cells—Fundamentals, Technology and Applications, vol. 3, John Wiley & Sons, 2003, p. 538.
[16] J. Lin, J.K. Lee, M. Kellner, R. Wycisk, P.N. Pintauro, J. Electrochem. Soc. 153 (2006) A1325.
[17] A.P. Saab, F.H. Garzon, T.A. Zawodzinski, J. Electrochem. Soc. 150 (2003) A214.
[18] E. Store, http://www.epson.com/cgi-bin/Store/consumer/consDetail.jsp.